

Trapped-electron runaway effect

E. Nilsson¹†, J. Decker², N. J. Fisch³ and Y. Peysson¹

¹CEA, IRFM, F-13108 Saint-Paul-lez-Durance, France

²Ecole Polytechnique Fédérale de Lausanne (EPFL), Centre de Recherches en Physique des Plasmas (CRPP), CH-1015 Lausanne, Switzerland

³Princeton Plasma Physics Laboratory, Princeton University, Princeton, NJ 08543, USA

(Received 1 March 2015; revised 27 March 2015; accepted 31 March 2015;
first published online 28 April 2015)

In a tokamak, trapped electrons subject to a strong electric field cannot run away immediately, because their parallel velocity does not increase over a bounce period. However, they do pinch toward the tokamak center. As they pinch toward the center, the trapping cone becomes more narrow, so eventually they can be detrapped and run away. When they run away, trapped electrons will have a very different signature from circulating electrons subject to the Dreicer mechanism. The characteristics of what are called *trapped-electron runaways* are identified and quantified, including their distinguishable perpendicular velocity spectrum and radial extent.

1. Introduction

Under acceleration by a constant toroidal electric field, circulating electrons in tokamaks run away when their velocity parallel to the magnetic field is so large that the frictional collision forces become too small to impede acceleration by the electric field. The runaway velocity is the demarcation velocity: the electric field cannot prevent electrons slower than this velocity from slowing down further due to collisions; collisions are too weak to prevent electrons faster than this velocity from undergoing acceleration by the electric field to even higher energies. This demarcation velocity is called the critical velocity (Dreicer 1959). However, since collisions are random events, it is not quite precisely put to term an electron as a runaway or not. A more precise description would be to assign to each electron a probability of running away, based on its initial set of coordinates (Fisch 1986; Karney and Fisch 1986). To the extent that this probability is a sharp function of velocity, the notion of a critical velocity then becomes useful.

Runaway electrons are sensitive, in addition to collisions, to other energy loss mechanisms such as the synchrotron radiation reaction force (Stahl et al. 2013). They are also sensitive to perturbation of the magnetic field, which lead to enhanced transport (Zeng et al. 2013). In addition, the runaway population that would arise in a tokamak magnetic field configuration is diminished owing to magnetic trapping effects in a non-uniform magnetic field, since trapped electrons cannot immediately contribute to the runaway electron population (Nilsson et al. 2015). The fate of the suprathermal electrons, whether trapped or circulating, is determined from the balance of the accelerating electric field and various radiative, convective and diffusive loss mechanisms.

† Email address for correspondence: emelie.nilsson@cea.fr

Runaway populations can be quite deleterious to the operation of a tokamak. In the case of a disruption, the loop voltage spikes, so that large numbers of runaway electrons reach relativistic velocities and damage the tokamak wall. Various means of mitigating the runaway damage have been suggested, since concerns are increasing as tokamaks become larger and carry more current, like in ITER (Hender et al. 2007; Izzo et al. 2011; Paz-Soldan et al. 2014). It is clearly important to understand the behavior of the runaway electrons in order to optimize a runaway electron mitigation strategy.

The runaway electron population in tokamaks typically arises from the acceleration of electrons with large parallel velocities, on the order of the critical velocity, and average perpendicular velocities, on the order of the thermal velocity. These electrons born via the Dreicer mechanism are circulating. In addition, a knock-on collision between an existing runaway and slow electrons can result in two runaway electrons. This secondary runaway generation process can generate an avalanche of runaway production and dominate the Dreicer effect, in particular during disruptions. These large angle collisions between runaways and slow electrons can result in electrons with perpendicular energies on the order of the parallel energies. When the knock-on runaways are created near the magnetic axis, trapped particle effects are not important (Rosenbluth and Putvinski 1997; Parks et al. 1999; Eriksson and Helander 2003). However, these electrons will be trapped if they are created far enough away from the magnetic axis. In fact, since circulating runaway electrons tend to move substantially radially outwards as they are accelerated by the electric field (Guan et al. 2010), the secondary electrons generated via collision with these runaways may not be near the magnetic axis at all and could be trapped. Alternatively, a significant population of suprathreshold trapped electrons can be generated via interaction with electron cyclotron waves.

The present paper focuses on electrons with a large enough parallel velocity to run away in a tokamak, but are magnetically trapped because of their large perpendicular velocity, and therefore incapable of running away. These trapped electrons drift radially inwards due to the Ware pinch (Ware 1970). Nearer the magnetic axis the trapping cone contracts such that these electrons could be detrapped and run away. When they run away, they will have a distinct signature, which is identified in this work.

The paper is organized as follows: In Sec. 2, we describe how trapped runaways are generated and provide their phase-space characteristics. In Sec. 3, we discuss collisional effects on the trapped runaways. In Sec. 4, we offer perspectives on runaway positrons and runaway interaction with RF current drive.

2. Signature of trapped runaways

Let us describe more precisely the expected signature of the trapped runaways. As opposed to circulating electrons, trapped electrons cannot run away while they remain on the same flux surface, because their interaction with the electric field results in no net gain in parallel velocity over a bounce period. However, according to the conservation of canonical angular momentum, they pinch toward the tokamak center. As they pinch toward the center, the trapping condition changes such that eventually they do run away. We call this the *trapped-electron runaway effect*, by which we refer to electrons that were initially trapped, before running away. However, when they do run away, trapped electrons will have a very different signature from the circulating electrons that run away in several ways.

First, the initially-trapped runaway electrons will run away closer to the magnetic axis of the tokamak than they were initially. Second, the trapped electron runaways will have a distinct pitch angle corresponding to the detrapping condition at the radial location where they run away, which implies a high-perpendicular velocity on the order of the critical velocity. In addition, upon application of a DC electric field these initially trapped electrons first need to undergo the Ware pinch and associated detrapping before running away. This process creates a delay in the runaway generation process, which can occur only if not disrupted by collisions or other mechanisms in the meantime.

For an initially Maxwellian distribution function, the fraction of trapped-electron runaways compared to Dreicer runaways would be small, although it increases with the effective charge. However, the relative importance of trapped-electron runaways might increase significantly for three reasons: first, the usual runaways may not be well confined, whereas, the trapped-electron runaways, since born nearer the magnetic axis, are very well confined; second, knock-on collisions between existing runaways and thermal electrons produce a non-thermal population of secondary runaways of which a significant number may be trapped due to their high-perpendicular velocities (Nilsson et al. 2015). Third, tokamak plasmas are typically non-Maxwellian, and a significant population of suprathermal electrons with high-perpendicular momentum can be created, for instance, via resonant interaction with electron cyclotron waves.

Assuming a circular plasma and neglecting the radial excursion of electron orbits, the unperturbed motion of an electron guiding center can be characterized by its radial position r , its momentum p , and the value ξ_0 of its pitch angle cosine $\xi = p_{\parallel}/p$ on the outboard midplane where $\theta = 0$ and the magnetic field is at a minimum. Here p_{\parallel} is the momentum projected in the direction of the magnetic field. Electron trapping derives from the adiabatic invariance of the magnetic moment $\mu = p^2(1 - \xi^2)/(2mB)$ along the particle orbit, such that electrons in a non-uniform magnetic field $B(r, \theta) = B_0(r)/(1 + \epsilon \cos \theta)$ are trapped if $|\xi_0| < \xi_T(r)$ with

$$\xi_T(r) = \sqrt{\frac{2\epsilon}{1 + \epsilon}},$$

where $\epsilon = r/R_0$ is the local inverse aspect ratio.

Due to the conservation of toroidal canonical momentum in an axisymmetric configuration, all trapped particles orbits subject to a toroidal electric field E_{ϕ} drift toward the plasma center according to the Ware pinch (Ware 1970)

$$\frac{dr}{dt} = -\frac{E_{\phi}}{B_{\theta}}, \quad (2.1)$$

where B_{θ} is the poloidal magnetic field. An otherwise unperturbed electron initially trapped on the flux surface r with $|\xi_0| < \xi_T(r)$ will drift inwards to the surface r' where $\xi_T(r') = |\xi_0|$. There, it will be detrapped and can run away if its parallel velocity is above the critical value. The electron will thus become circulating at the radial location ϵ' with

$$\epsilon' = \frac{\xi_0^2}{2 - \xi_0^2}. \quad (2.2)$$

Figure 1 shows the required displacement $\Delta\epsilon = \epsilon - \epsilon'$ and Fig. 2 shows the radial position ($\epsilon' = r/R$) where the electrons can detrap and run away.

Runaway electrons born at a given radial location via this detrapping process driven by the Ware pinch will have a specific pitch-angle according to the local trapping

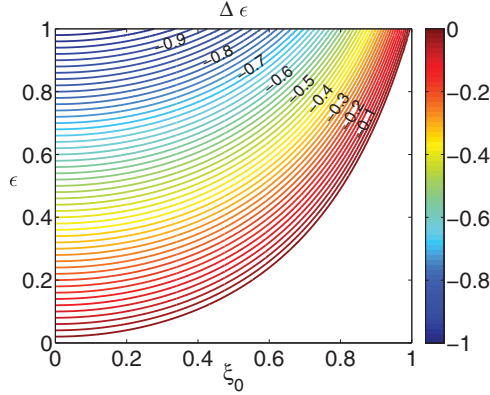


FIGURE 1. The inward radial displacement ($\Delta\epsilon$) required for trapped electron initially at radial position ϵ and pitch angle ξ_0 to become circulating.

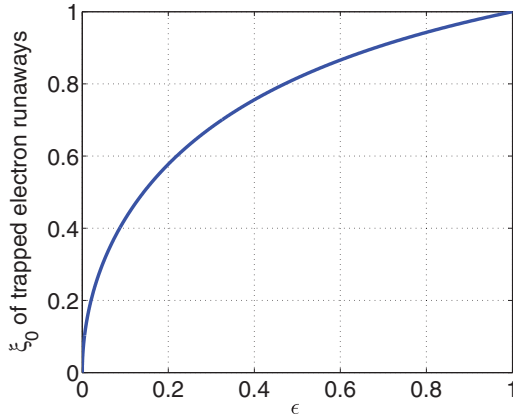


FIGURE 2. The trapped-electron runaways will appear with a distinct pitch angle (ξ_0) in the radial direction.

condition. The minimum perpendicular velocity of the trapped electron runaways is presented in Fig. 3, normalized to $v_c(\xi_0 = 1)$. The time it takes for these initially trapped electrons to become runaways is derived from the Ware pinch velocity and radial displacement until detrapping occurs

$$dt_W = \frac{B_\theta}{E_\phi} R \left(\epsilon - \frac{\xi_0^2}{2 - \xi_0^2} \right). \quad (2.3)$$

For an equilibrium with $B_\theta = 0.05$ T and $E_\phi = 0.8$ Vm⁻¹. The time required for a trapped electron to become passing is shown in Fig. 4.

In a disruption in an ITER-like scenario the toroidal electric field can be much stronger; around 38 Vm⁻¹ has been predicted (Hender et al. 2007). In that case, the Ware pinch detrapping time scale would be much shorter; see Fig. 5.

Corrections to the detrapping radius and detrapping time due to the Shafranov shift, non-circular plasma shape, grad-B and curvature drifts are beyond the scope of this paper. It is important to note that very near the magnetic axis the approximations made in this paper break down.

Although the poloidal magnetic field B_θ has little effect on the detrapping condition, it does have a strong effect on the detrapping time. For simplicity, we took the E_ϕ/B_θ

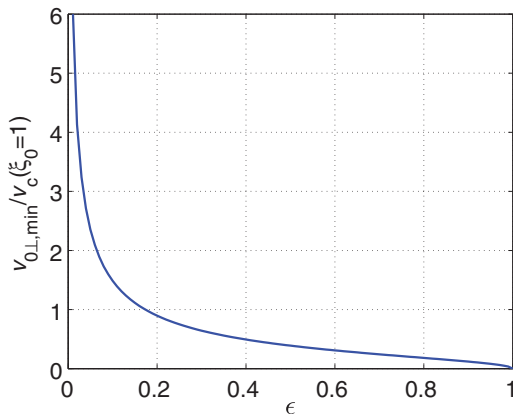


FIGURE 3. The radial distribution of the minimum perpendicular velocity of the trapped electron runaways, normalized to the critical velocity for $\xi_0 = 1$.

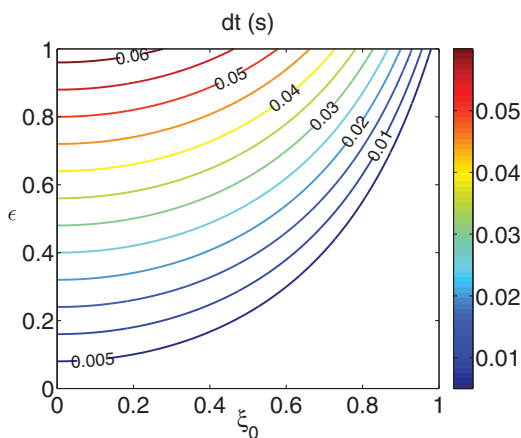


FIGURE 4. Time (s) for trapped electrons at (ξ_0, ϵ) to reach the radial position where they become passing electrons, for $B_\theta = 0.05$ T, $E_\phi = 0.8$ Vm $^{-1}$ and $R = 1$ m.

velocity to be constant. In fact, as the electron pinches inward, the poloidal field decreases, thereby speeding up the drift. Thus, a more precise formulation of (2.3) would account for the E_ϕ/B_θ dependence upon r .

3. Limitations of the collisionless approach

The collisionless approximation used in Sec. 2 is valid if the pinch time is small compared to both the collisional slowing down and detrapping times of runaway electrons. If the pinch time is longer than the slowing-down time, the electron may slow down such that it may not have the energy required to run away when it finally detraps. If the electron undergoes significant pitch-angle scattering during the pinch time, it may be detrapped at a different radial location.

Since the collision time increases with velocity, the validity condition for the collisionless approach must be evaluated from the pitch angle dependent critical momentum (Rosenbluth and Putvinski 1997)

$$p_c^2 \approx \frac{2}{1 + \xi_0} \frac{E_c}{E}, \quad (3.1)$$

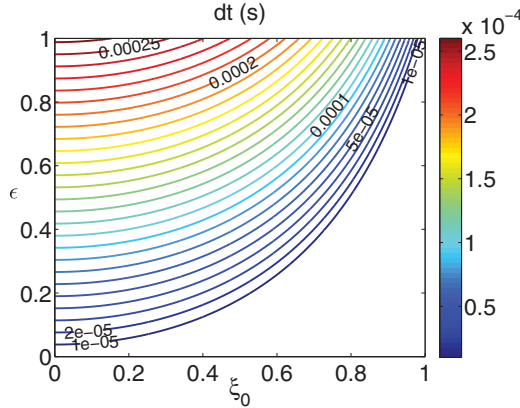


FIGURE 5. Time (s) for trapped electrons at (ξ_0, ϵ) to reach the radial position where they become passing electrons, for $B_\theta = 0.01$ T, $E_\phi = 38$ V m $^{-1}$ and $R = 1$ m.

where the critical field E_c is proportional to the plasma density. The slowing-down time for electrons with velocity $v_c/c = p_c/\gamma_c$ is

$$\tau_c = \frac{4\pi\epsilon_0^2 m_e^2 v_c^3}{q^4 n_e \ln \Lambda}.$$

Slowing-down can thus be neglected if $dt_w \ll \tau_c$.

Collisional detrapping via pitch-angle scattering occurs over a shorter time than the collision time that is proportional to the square of the width ξ_T of the trapping region and can be estimated as

$$\tau_{dt} \sim \frac{\epsilon \tau_c}{1 + Z_{\text{eff}}}.$$

If the condition $dt_w \ll \tau_{dt}$ is not satisfied, trapped-electron runaways will still be generated, but the detrapping radial distribution will be different.

The collisionless condition is shown in Fig. 6 for ITER-like parameters and various values of the electric field. The density is $n_e = 10^{20}$ m $^{-3}$. The magnetic field is calculated from a current density profile, peaked on-axis and with a total plasma current of $I_p = 15$ MA. With the current profile assumed in this calculation, the maximum of the poloidal magnetic field is located inward from the plasma edge, which explains the maximum in the energy condition. The radial dependence of the density and the electric field strength are not taken into account.

The minimum energy required for the collision time to be longer than the Ware pinch time is on the order of MeV for ITER-like parameters during a disruption. Considering that runaway electrons have many tens of MeV, it can be expected that runaways produced from knock-on collisions should be in the range where collisions can be neglected. For trapped electron runaways with lower energy, collisions must be accounted for. That regime is left for a future study.

Just like the collisional slowing down, the synchrotron reaction force (Pauli 1958) limits the energy of the particle.

The relativistic characteristic time for the radiation reaction force is

$$\tau_r = \frac{6\pi\epsilon_0\gamma(m_0c)^3}{q^4 B^2} \approx 5.2 \frac{\gamma}{Z^4 B^2}. \quad (3.2)$$

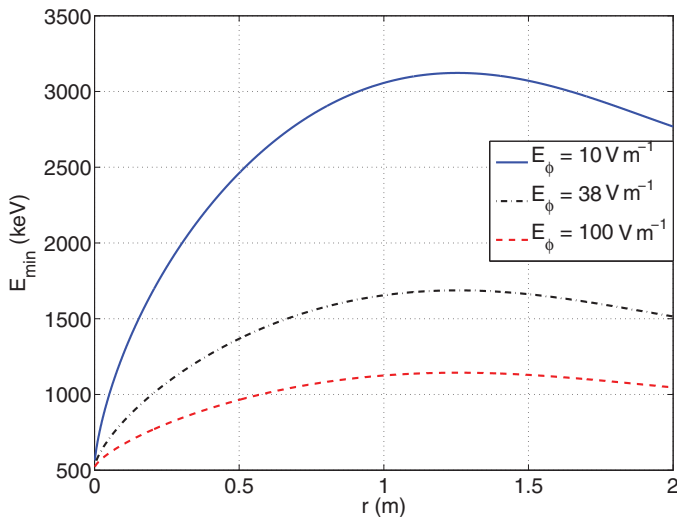


FIGURE 6. The minimum energy needed for the Ware pinch to be faster than the collision time, for the parameters $E_\phi = 10 \text{ Vm}^{-1}$, 38 Vm^{-1} and 100 Vm^{-1} , $n_e = 10^{20} \text{ m}^{-3}$ and $R = 6.2 \text{ m}$. The poloidal magnetic field is calculated from a current density profile with a total plasma current of $I_p = 15 \text{ MA}$.

In addition the synchrotron reaction force limits the pitch angle $\theta = \arccos(\xi)$ (Helander et al. 2002)

$$F_{\text{rad}, \xi} = -\frac{p\xi\sqrt{1-\xi^2}}{\gamma\tau_r}. \quad (3.3)$$

This force could affect the trapped electron runaways in the Ware pinch process, as electrons would detrapp faster, i.e. at a larger radius than predicted in Sec. 2, if p_\perp/p_\parallel decreases.

Limitations of the collisionless theory was discussed previously in this section and a regime was identified where the Ware pinch detrapps trapped runaways fast enough for the collisions to be negligible ($dt_w \ll \tau_c$). A similar condition can be set for the radiation loss time $dt_w \ll \tau_r$. We compare the time scale of collisional damping with the one of the radiation damping

$$\frac{\tau_c}{\tau_r} = \frac{2\epsilon_0}{3m_e n_e \ln \Lambda} \gamma \left(\frac{v}{c}\right)^3 Z^4 B^2 \approx \frac{\gamma}{n_{e,19}} \left(\frac{v}{c}\right)^3 Z^4 B_{[5T]}^2, \quad (3.4)$$

where $n_{e,19}$ is the electron density in the unit 10^{19} m^{-3} and $B_{[5T]}$ in units of 5 T. For relevant plasma parameters, the condition $\tau_c \ll \tau_r$ is fulfilled unless γ gets very large. From the minimum energy defined in Fig. 6, where the Lorentz factor γ is in the range of 1–6, for higher γ the time scale of the synchrotron reaction force may be short enough to change the pitch before the detrapping radius is reached, if the product $B^2 Z^4/n_e$ becomes large. Since this effect would speed up the detrapping process, the prediction in Sec. 2 can be considered as an upper estimate of the detrapping time and lower estimate of the detrapping radius. To properly account for the combined effect of synchrotron reaction and collisional drag on the trapped-electron runaway distribution during the Ware pinch would require further investigation by numerical studies.

4. Discussion

This paper describes how initially trapped electrons may become runaway electrons if their parallel velocity is above the critical runaway velocity as they become detrapped following the inward Ware pinch. These runaway electrons are born nearer the magnetic axis as compared to their initial location, and with a high-perpendicular velocity corresponding to the trapped/circulating boundary. That will distinguish the trapped runaways from the passing runaways, which have average perpendicular energies. They will produce a relatively more intense synchrotron radiation than Dreicer runaways. The production dynamics of the trapped-electron runaways is determined by the Ware pinch time. There will be a turn-on time for the electrons to reach the radial detrapping position and only then to begin to run away. The presence of trapped-electron runaways may affect the radial profile of runaway electrons since they are concentrated near the magnetic axis. Even in the case where primary generation would be small in the center, for example for very peaked density, one could still expect a centrally concentrated runaway electron population under some circumstances. This would be the case if the avalanche growth rate from knock-on collisions decays strongly off-axis owing to magnetic trapping effects as found for toroidal geometries (Nilsson et al. 2015). At the same time, the trapped-electron runaways are concentrated near the center, as found in the previous section.

In other words, the radial dependence of the growth rate of runaways depends on various effects, where the avalanche effect and the trapped-electron runaway effect would weigh the runaway distribution toward the center. Quantitative predictions of the radial profile of runaway electrons are left to future studies. All these signatures should be most prominent during a disruption, where the electric field is large, and might be used to provide information on plasma conditions. The combination of high synchrotron emission and specific dynamics could make it possible to identify the signature of trapped-runaway electrons during disruptions when a large number of energetic trapped electrons is generated via knock-on collisions.

The large perpendicular energies of the trapped-electron runaways also suggest that they may be easier to control than conventional Dreicer runaways, as they can be deconfined through interactions with ripple fields (Laurent and Rax 1990; Rax et al. 1993), coherent wave instabilities (Fülöp et al. 2006; Fülöp and Newton 2014) or magnetic perturbations (Papp et al. 2011). In all of these processes, the strength of the interaction increases with perpendicular momentum.

Recently, there has been interest in the creation of runaway positrons in tokamaks, and the information that might be obtained from them upon annihilation (Helander and Ward 2003; Fülöp and Papp 2012; Liu et al. 2014). When large tokamaks disrupt, large electron–positron pair production is expected to occur. The positron runaways behave just like electron runaways, only they run away in the opposite direction. Just as there are circulating positron runaways, there will be trapped positron runaways. These trapped positron runaways will pinch toward the tokamak magnetic axis just like the trapped electron runaways. Except that they will travel in the opposite toroidal direction, which will affect the Doppler shift of the synchrotron radiation, the trapped positron runaways will have a completely analogous signature to the trapped electron runaways. Moreover, since the positrons would only be produced in large numbers through the avalanche effect involving very high energy runaways, there will be relatively more of the trapped positron runaways (compared to the usual positron runaways) than there would be trapped electron runaways (compared to the usual electron runaways). This effect would be enhanced to the extent that the

most energetic runaways – and those most capable of the pair production – would be found near the low field side of the tokamak (Guan et al. 2010), where the trapping effect is also most significant.

Note that the trapped-electron runaway effect that we discuss is for runaway electrons that run away eventually in the direction in which they support the plasma current. The same is true for the runaway positrons. When the tokamak current is maintained by a DC electric field, it is after all the thermal electrons that carry the toroidal current, and the runaway electrons carry current in the same direction, only they are accelerated to far higher energies. This would also be true during start-up of the tokamak (Mueller 2013), if the start-up relies on an inductive current. In such a case, there is also danger from runaway electrons, since the plasma may not be so dense as to hold back the runaways. Moreover, in the case of RF-assisted start-up of the current, such as through electron cyclotron heating, there might be more electrons produced at higher energies, which could then run away in the direction in which the runaways support the current.

Whether or not the runaways are in a direction to support the plasma current is an important distinction that comes into play in non-inductive start-up of the tokamak current. In the case of non-inductive current drive, for example by RF waves (Fisch 1987), there is the opportunity to start up the tokamak or to recharge the transformer (Fisch 2010). In such a case, the loop voltage is driven negative; in other words, as the RF-current is increased, a loop voltage is induced which opposes the RF-driven current. This DC electric field also produces runaway electrons, only now they are so-called *backwards runaways*, which are runaway electrons that carry current counter to the toroidal current (Fisch 1986; Karney and Fisch 1986). It is also important to note that the trapped-electron runaways are not a concern in the case of backward runaways. In this case, which may occur during the startup or flattop phases in the presence of strong RF current drive (Karney et al. 1985; Fisch 1987, 2010; Ding et al. 2012; Li et al. 2012), the electric field opposes the plasma current such that the pinch is directed outward where the trapping cone widens. Hence, in the case of RF ramp-up, while circulating backwards runaways are produced, there is no production whatsoever of backwards trapped-electron runaways (or, for the same reason, backwards trapped-positron runaways). Thus, in vigorous RF ramp-up regimes, while the circulating backwards runaways might be of some concern, at least the trapped-electron runaways do not add to that concern.

A recurring question is to what extent RF current drive generates runaway electrons. This question should also be posed for the trapped-electron runaways. In the case of RF current drive, if the current drive effect relies on RF wave interactions with suprathermal electrons, there is risk of producing runaway electrons. It is particularly the case for lower hybrid current drive (Fisch 1978), where a suprathermal electron tail is formed at high parallel velocities that could supply more runaway electrons than could a Maxwellian distribution. It is also the case for electron cyclotron current drive (Fisch and Boozer 1980), where heating in perpendicular velocity makes electrons collide less frequently and become more likely to run away. In these cases, the RF heating of passing electrons enhances the runaway current through the usual runaway effect. However, there is also a trapped particle runaway effect when the RF current drive affects trapped electrons. Consider first waves that provide parallel momentum to energetic trapped electrons, such as low parallel-phase-velocity waves (Wort 1971). Since the particles remain trapped, there is an RF-pinch effect similar to the Ware pinch effect (Fisch and Karney 1981). If the wave momentum is in the direction supportive of the total current, then as with the Ware pinch effect,

the pinch will be inwards. Moreover, as with the Ware pinch, the trapped electrons experience less stringent trapping conditions when they pinch, so they can eventually run away like a trapped runaway. One important difference is that, as opposed to the Ware pinch effect where the electric field pinches the electron, without increasing its energy, in the case of the RF-pinch effect, the RF waves pinch the electron, while increasing its energy. As a result, the trapped runaways become detrapped sooner, and so run away at larger radii. It must be pointed out that the RF pinch may only occur if the wave-particle resonance is present continuously through the pinching process, i.e. if the spatial distribution of the waves has sufficient radial extent. In any event, in inputting parallel momentum with waves that would be supportive of the toroidal current, whereas targeting electrons with higher parallel velocity can increase the number of runaway electrons, targeting electrons with low parallel velocity can increase the number of trapped runaways.

In contrast, in the case of perpendicular heating rather than parallel heating of trapped electrons, such as by electron cyclotron waves, there is no pinch effect bringing electrons to less stringent trapping conditions. In fact, the perpendicular heating causes the electrons to be more deeply trapped. Hence, there is no trapped-particle runaway effect for heating by electron cyclotron waves.

5. Summary

To sum up, we identified the trapped-electron runaway effect. We calculated the key parameters that distinguish these runaways, namely the large perpendicular energy, the dependency of the perpendicular energy on radius, and the turn-on time for the appearance of the runaways. We identified when these effects might be expected (in the case of positrons) and when they would be absent (in the case of RF ramp-up). Possible observables would therefore be based on signals sensitive to perpendicular energy, such as synchrotron radiation. Similarly, the degree of manipulation by waves or magnetic perturbations is also sensitive to perpendicular energy. Thus, we hope that these observations and calculations will assist in formulating methods of controlling those runaways or in utilizing measurements of their behavior for informing on other processes in the plasma.

Acknowledgements

This work has been carried out within the framework of the EUROfusion Consortium and has received funding from the Euratom research and training programme 2014–2018 under grant agreement No. 633053. The views and opinions expressed herein do not necessarily reflect those of the European Commission. The authors appreciate the hospitality of the Chalmers University of Technology, where, at a meeting organized by Professor Tünde Fülöp, these ideas were initially conceived. The authors are grateful to Eero Hirvijoki, Isztvan Pusztai and Adam Stahl for fruitful discussions. One of us (NJF) acknowledges support, in part, from DOE Contract No. DE-AC02-09CH11466.

REFERENCES

- Ding, B. J. et al. 2012 Current ramp-up with lower hybrid current drive in EAST. *Phys. Plasmas* **19**(12), 122 507.
- Dreicer, H. 1959 Electron and ion runaway in a fully ionized gas. I. *Phys. Rev.* **115**(2), 238–249.

- Eriksson, L. G. and Helander, P. 2003 Simulation of runaway electrons during tokamak disruptions. *Comput. Phys. Commun.* **154**, 175–196.
- Fisch, N. J. 1978 Confining a tokamak plasma with RF-driven currents. *Phys. Rev. Lett.* **41**(13), 873–876.
- Fisch, N. J. 1986 Transport in driven plasmas. *Phys. Fluids* **29**(1), 172–179.
- Fisch, N. J. 1987 Theory of current drive in plasmas. *Rev. Mod. Phys.* **59**(1), 175–234.
- Fisch, N. J. 2010 Transformer recharging with alpha channeling in tokamaks. *J. Plasma Phys.* **76**(3-4), 627–634.
- Fisch, N. J. and Boozer, A. H. 1980 Creating an asymmetric plasma resistivity with waves. *Phys. Rev. Lett.* **45**(9), 720–722.
- Fisch, N. J. and Karney, C. F. F. 1981 Current generation with low-frequency waves. *Phys. Fluids* **24**(1), 27–39.
- Fülöp, T. and Newton, S. 2014 Alfvénic instabilities driven by runaways in fusion plasmas. *Phys. Plasmas* **21**(8), 080702.
- Fülöp, T. and Papp, G. 2012 Runaway positrons in fusion plasmas. *Phys. Rev. Lett.* **108**(21), 225003.
- Fülöp, T., Pokol, G., Helander, P. and Lisak, M. 2006 Destabilization of magnetosonic-whistler waves by a relativistic runaway beam. *Phys. Plasmas* **13**(6), 062506.
- Guan, X., Qin, H., and Fisch, N. J. 2010 Phase-space dynamics of runaway electrons in tokamaks. *Phys. Plasmas* **17**, 092502.
- Helander, P., Eriksson, L.-G. and Andersson, F. 2002 Runaway acceleration during magnetic reconnection in tokamaks. *Plasma Phys. Control. Fusion* **44B**, 247–262.
- Helander, P. and Ward, D. J. 2003 Positron creation and annihilation in tokamak plasmas with runaway electrons. *Phys. Rev. Lett.* **90**(13), 135004.
- Hender, T. C. et al. 2007 MHD stability, operational limits and disruptions. *Nuclear Fusion* **47**, S128–S202.
- Izzo, V. A. et al. 2011 Runaway electron confinement modelling for rapid shutdown scenarios in DIII-D, Alcator C-Mod and ITER. *Nuclear Fusion* **51**, 063032.
- Karney, C. F. F. and Fisch, N. J. 1986 Current in wave-driven plasmas. *Phys. Fluids* **29**(1), 180–192.
- Karney, C. F. F., Fisch, N. J. and Jobes, F. C. 1985 Comparison of the theory and the practice of lower-hybrid current drive. *Phys. Rev. A* **32**(4), 2554–2556.
- Laurent, L. and Rax, J. M. 1990 Stochastic-instability of runaway electrons in tokamaks. *Europhys. Lett.* **11**(3), 219–224.
- Li, M., Ding, B., Li, W., Kong, E., Shan, J., Liu, F., Wang, M. and Xu, H. 2012 Investigation of LHCD efficiency and transformer recharging in the EAST tokamak. *Plasma Sci. Technol.* **14**(3), 201–206.
- Liu, J., Qin, H., Fisch, N. J., Teng, Q. and Wang, X. 2014 What is the fate of runaway positrons in tokamaks? *Phys. Plasmas* **21**, 064503.
- Mueller, D. 2013 The physics of tokamak start-up. *Phys. Plasmas* **20**(5), 058101.
- Nilsson, E., Decker, J., Peysson, Y., Granetz, R. S., Saint-Laurent, F. and Vlaminic, M. 2015 Kinetic modelling of runaway electron avalanches in tokamak plasmas. *Plasma Phys. Control. Fusion*. Submitted For Publication.
- Papp, G., Drevlak, M., Fülöp, T., Helander, P. and Pokol, G. I. 2011 Runaway electron losses caused by resonant magnetic perturbations in ITER. *Plasma Phys. Control. Fusion* **53**(9), 095004.
- Parks, P. B., Rosenbluth, M. N. and Putvinski, S. V. 1999 Avalanche runaway growth rate from a momentum-space orbit analysis. *Phys. Plasmas* **6**(6), 2523–2528.
- Pauli, W. 1958 *Theory of Relativity*. New York: Dover Publications.
- Paz-Soldan, C. et al. 2014 Growth and decay of runaway electrons above the critical electric field under quiescent conditions. *Phys. Plasmas* **21**(2), 022514.
- Rax, J. M., Fisch, N. J. and Laurent, L. 1993 Fast particle resonances in tokamaks. *Plasma Phys. Control. Fusion* **35**(B), B129–B140.
- Rosenbluth, M. N. and Putvinski, S. V. 1997 Theory for avalanche of runaway electrons in tokamaks. *Nuclear Fusion* **37**(10), 1355–1362.

- Stahl, A., Landreman, M., Papp, G., Hollmann, E. and Fülöp, T. 2013 Synchrotron radiation from a runaway electron distribution in tokamaks. *Phys. Plasmas* **20**, 093 302.
- Ware, A. A. 1970 Pinch effect for trapped particles in a tokamak. *Phys. Rev. Lett.* **25**(1), 15–17.
- Wort, D. J. H. 1971 The peristaltic tokamak. *Plasma Phys.* **13**(3), 258–262.
- Zeng, L. et al. and the TEXTOR team 2013 Experimental observation of a magnetic-turbulence threshold for runaway-electron generation in the TEXTOR tokamak. *Phys. Rev. Lett.* **110**, 235 003.